



## Eccentric Loading of Helical Piers™ for Underpinning

Gary Seider

Senior Engineer, A.B. Chance Company, Centralia, Missouri

**SYNOPSIS** Over the last six years, Helical Piers have been utilized as compression members in the remedial repair of residential and light commercial structures. Current installation techniques create a small offset between the pier shaft and the grade beam or footing being underpinned. The purpose of this study was to examine the effects of the eccentric load that is applied to the top of the shaft on the Helical Pier. Three different sizes of piers were installed at a building site where the soil is predominantly clay. Compressive loads were applied, and data was recorded from which bending moments versus depth, stress distributions, and angular deflections at the top of the shaft were developed. Results show Helical Pier behavior compares with piles under lateral loading conditions. The specific loads required will determine which pier type to use.

### INTRODUCTION

Helical Piers, also known as screw anchors, consist of one or more helically shaped circular steel plates attached to a central steel shaft. The pier can consist of only one shaft with affixed helical plates, or it can have any number of shaft extensions coupled together to form a long continuous pier. Helical Piers are installed into soil by applying torque to the pier head.

Screw anchors have been used extensively over the last 30 years for the construction and stabilizing of electrical transmission and distribution structures. The primary application and design was for tension (uplift) forces. Helical piers of the same type are presently being used as compression members in the remedial repair of residential and light commercial structures. These compression loads are usually in the range of 6-15 kips. However, some applications can require compression loads exceeding 30 kips.

The uplift capacity of a helical pier has been empirically related to the torque required for installation (Clemence, Hoyt, 1989). This same relationship can be applied to the pier's compression capacity (Edwards, Rupiper, 1989). Using this relationship, Helical Piers can be installed to a torque level established by the required design load. Ultimate theoretical capacity for screw anchors can also be evaluated using the bearing capacity method. This can be done when soil strength parameters are available.

For underpinning, Helical Piers are installed as near to the side of the footing or grade beam of a building as possible. Generally, some type of site preparation is required. The footing usually needs to be chipped back and smoothed so that the pier can be attached to the face of the stem wall. Attachment to the stem wall is achieved through the use of a steel bracket or concrete haunch. Using present installation

techniques, it is not possible to install the pier so that it lies directly underneath the center of the footing and stem wall. The small offset between the shaft of the pier and the center of the footing causes eccentric compression loading.

The purpose of this study was to explore the effects of the eccentric load that is applied to the top of the shaft on the pier. The three Helical Pier types tested are currently being used in remedial underpinning.

### TEST SITE

The site chosen for this study was a section of perimeter wall (outside) of the shipping facility of the A. B. Chance Company in Centralia, Missouri. This site was chosen for its obvious location advantage, plus the building had sufficient dead and live loads as to eliminate any possibility of vertically lifting the building at the test site. The building also had a large footing which required minimal site preparation for the tests.

Two soil borings with Standard Penetration Test (SPT) blow counts were conducted. Shelby tube samples were taken at the approximate depth to which the helical plates on the anchors would be driven. Each boring was located about 10' from the building wall. The Helical Pier test sites were between the two boring sites. Table 1 summarizes the data acquired from the borings.

Each test site was dug immediately prior to pier installation. The bottom and outside face of the footing was chipped smooth using an impact tool. The footing was considered massive enough to transmit the eccentric load, so no more site preparation was required.

Table 1. Soil Boring Data

Depth (ft.)	Blows(N) B-1	Blows(N) B-2	W (%)	LL (%)	PL (%)	PI (%)	C (T/ft <sup>2</sup> )	ε (%)	γ <sub>d</sub> (lb/ft <sup>3</sup> )
6	4/6	2/2/3							
11	2/3/3	2/3/4							
16	3/4/6	3/4/5							
20	2/4/5	3/6/7							
22	2/3/6/6		▼ (Lab Test Data From Boring 2)						
23			16.2	31.6	11.1	20.5	1.42	17.3	116.0
25	4/6/9								
27			14.8	31.6	10.0	21.6	2.39	8.65	120.3
			▲ (Lab Test Data From Boring 1)						

HELICAL PIER DESCRIPTION AND INSTALLATION

The first Helical Pier type, trade name SS5, used two 10" diameter helical plates. The shaft material is a round cornered square with a dimension across the flats of 1 1/2". The helices were spaced about 4' apart for ease of installation. Normal spacing is typically three helix diameters. The SS5 pier was installed to a depth of about 24' as shown in the soil profile chart in Figure 1.

The second Helical Pier type, trade name SS150, used one 10" and one 12" diameter helical plate. The shaft material is a high strength round cornered square with a dimension across the flats of 1 1/2", the same as on the SS5. The helices were also spaced about 4' apart. The SS150 pier was installed to a depth of about 30' as shown in the soil profile chart in Figure 1.

The third Helical Pier type, trade name SS175, used two 14" diameter helical plates. The shaft material is a high strength round cornered square with a dimension across the flats of 1 3/4". The helices were spaced about 4' apart. The SS175 pier was installed to a depth of about 30' as shown in the soil profile chart in Figure 2.

All three piers were installed adjacent to the footing at an angle of about 3° from vertical. Torque versus depth was recorded continuously during installation, which was terminated at a predetermined torque. The last extension of each pier was instrumented with strain gages.

Monitoring torque was very important not only in pier capacity prediction, but also in ensuring that the applied torque did not peel strain gages off the shaft by exceeding the elastic limit of the shaft material. Table 2 lists the average torque over the last three feet of installation depth.

Table 2: Average Installation Torque

Pier Type	Average Torque(lb.-ft.)
SS5	1800
SS150	2933
SS175	4133

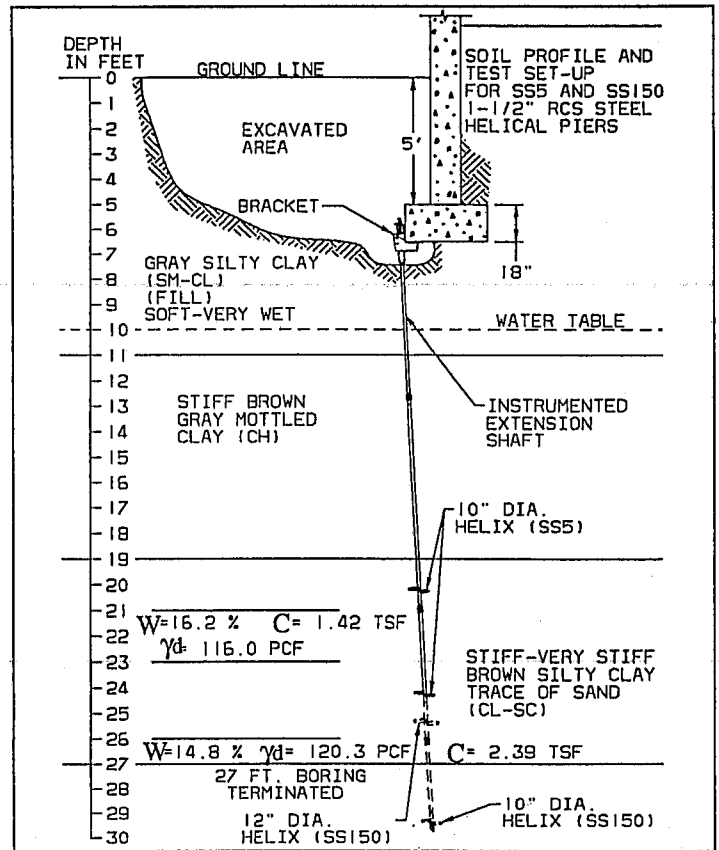


Fig. 1.

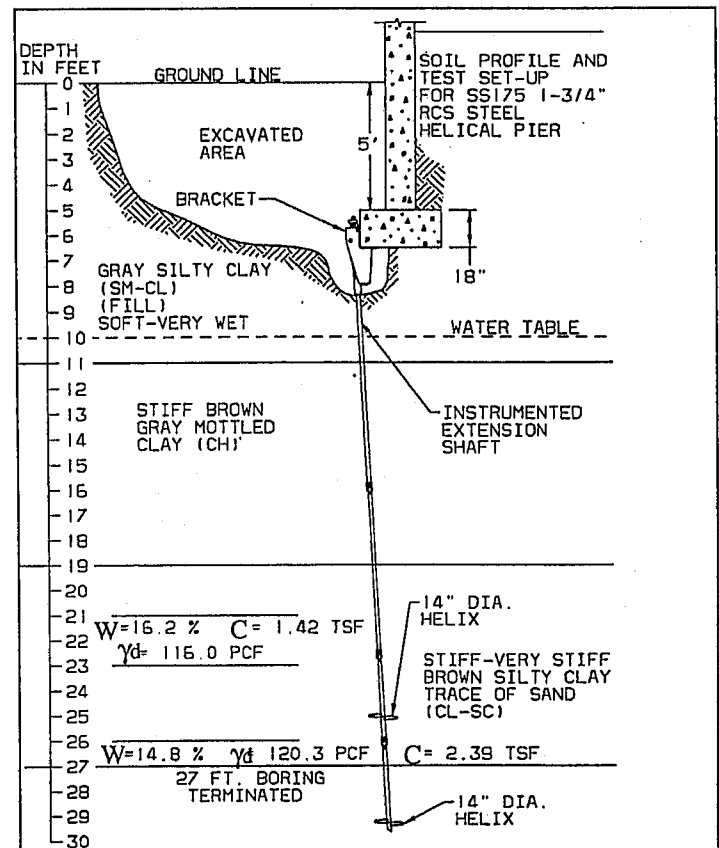


Fig. 2.

Equally important for pier installation was the orientation of the shaft with respect to the footing. Each pier was installed so that the shaft was oriented as shown in Figure 3a.

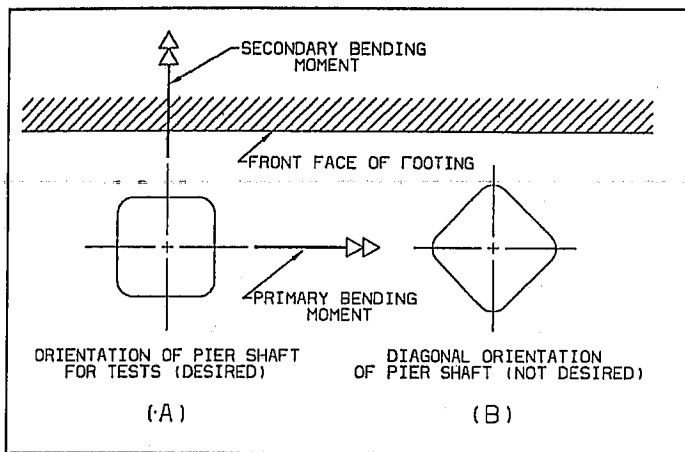


Fig. 3.

Orienting the pier shaft as in Figure 3b was not desired. The moment of inertia is the same for both orientations because the section is doubly symmetric. However, the section modulus is less for a shaft with diagonal orientation. This would result in a shaft with only 79% of the bending capacity at initial yield of a shaft oriented as in Figure 3a. Figure 3a also shows the orientation of the primary and secondary bending moments. The primary moment is developed as a result of the eccentric compressive load that was applied during load tests. The secondary bending moment is developed as a result of any minor misalignments occurring at the top of the pier during load tests.

After pier installation, a commercially available steel bracket was bolted to the footing and connected to the Helical Pier to complete the installation. The steel brackets used are designed to minimize the amount of angular deflection at the top of the pier.

Each excavation and subsequent installation was done on separate days during November and December 1991. Compressive loading was done on the same day as the installations.

### COMPRESSIVE LOAD TESTS

Compressive loads were applied directly to the bracket through the use of a calibrated hydraulic jack and jacking tool. Compressive loads were applied in increments of 2 to 3 kips. As each load point was achieved, the load was held long enough so that strain gage data could be recorded. Each pier had three strain gages located at each of four points along the last (top) extension. The gages were positioned on three faces of the pier shaft with each gage being centered and aligned with the longitudinal axis of the shaft. Wires connecting the strain gages to the conditioner and amplifier system were epoxied to the faces of the shaft for protection. Output was recorded using a chart recorder. Compressive loading contin-

ued until preselected load values were achieved for each anchor type. These preselected values were based on installation torque.

During compression loading, angular deflection data was also measured and recorded. Two dial indicators were rigidly attached to the footing. The indicator stems rested on a smooth flat plate that was rigidly attached to the bracket. As compressive loads were applied during testing, the dial indicators would display the amount of deflection or rotation of the bracket with respect to the footing of the building.

After tests, the bracket was removed to expose the pier shaft. The last (top) extension was then backed out and retrieved for examination. Any evidence of permanent bending damage was recorded.

All three Helical Piers were tested in this manner. The only difference between tests was the magnitude of the compressive load applied.

### TEST RESULTS

Strain gage data was tabulated and converted from volts to strain. From the strain data, axial loads and bending moments were calculated for each anchor type at every load applied. Figures 4, 5, and 6 show the test results for the SS5, SS150, and SS175 Helical Piers respectively. Each graph shows the load cases conducted in the field test and the corresponding moment-depth curve. The bending moment represented in the graph is the primary bending moment. The depth along shaft shown on the graph is the actual distance in inches from where the pier shaft leaves the steel bracket at the top, to a point just below the last strain gage position. Gage positions on the shaft are shown by horizontal lines bisecting the moment-depth curves.

Each moment-depth curve is a cubic spline with free ends fitted to points at each gage position for a given load case. As compressive loads increase, the primary moment also increases. The moments increase in the negative direction because the orientation of the moment is in the opposite direction to that shown in Figure 3.

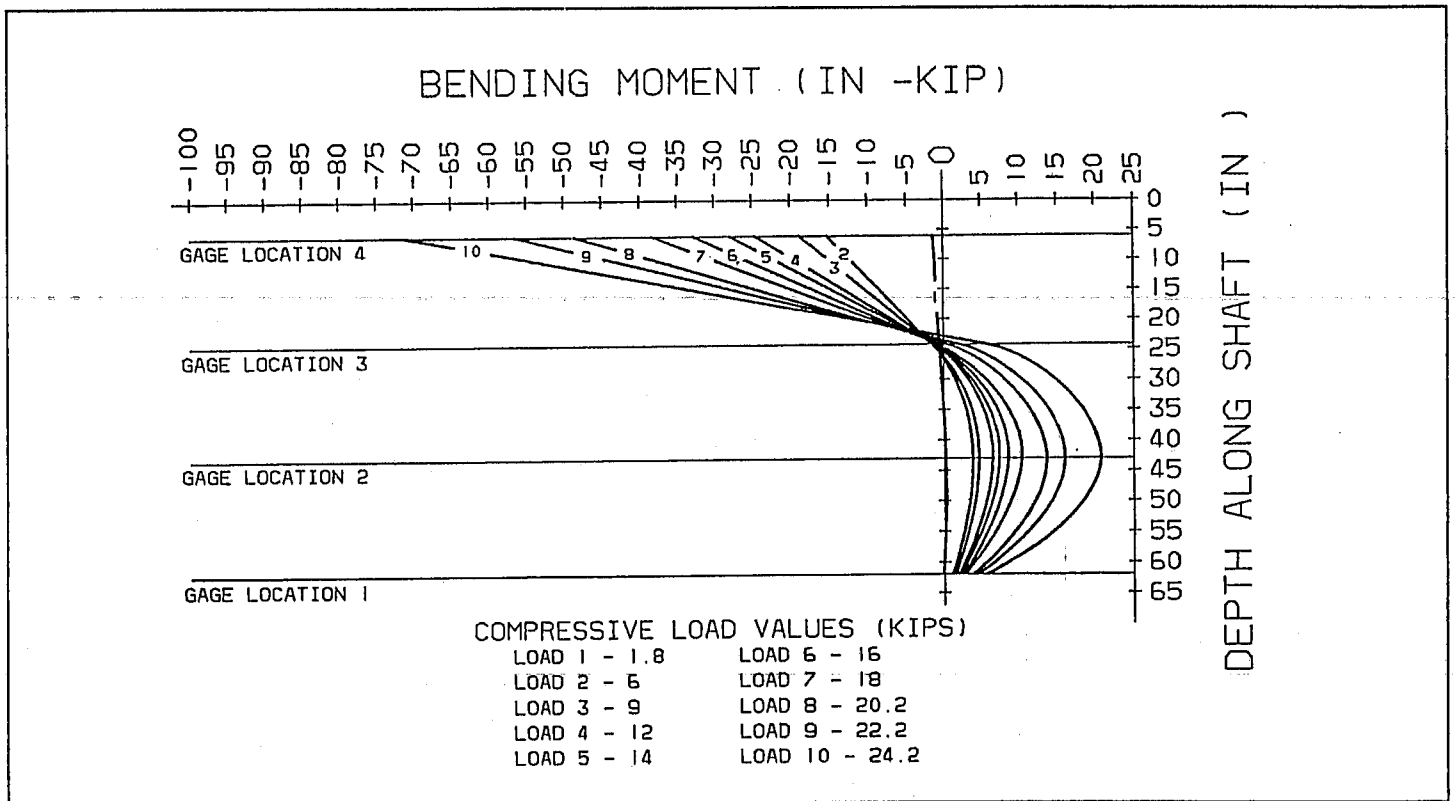


Fig. 4. SSHelical Pier

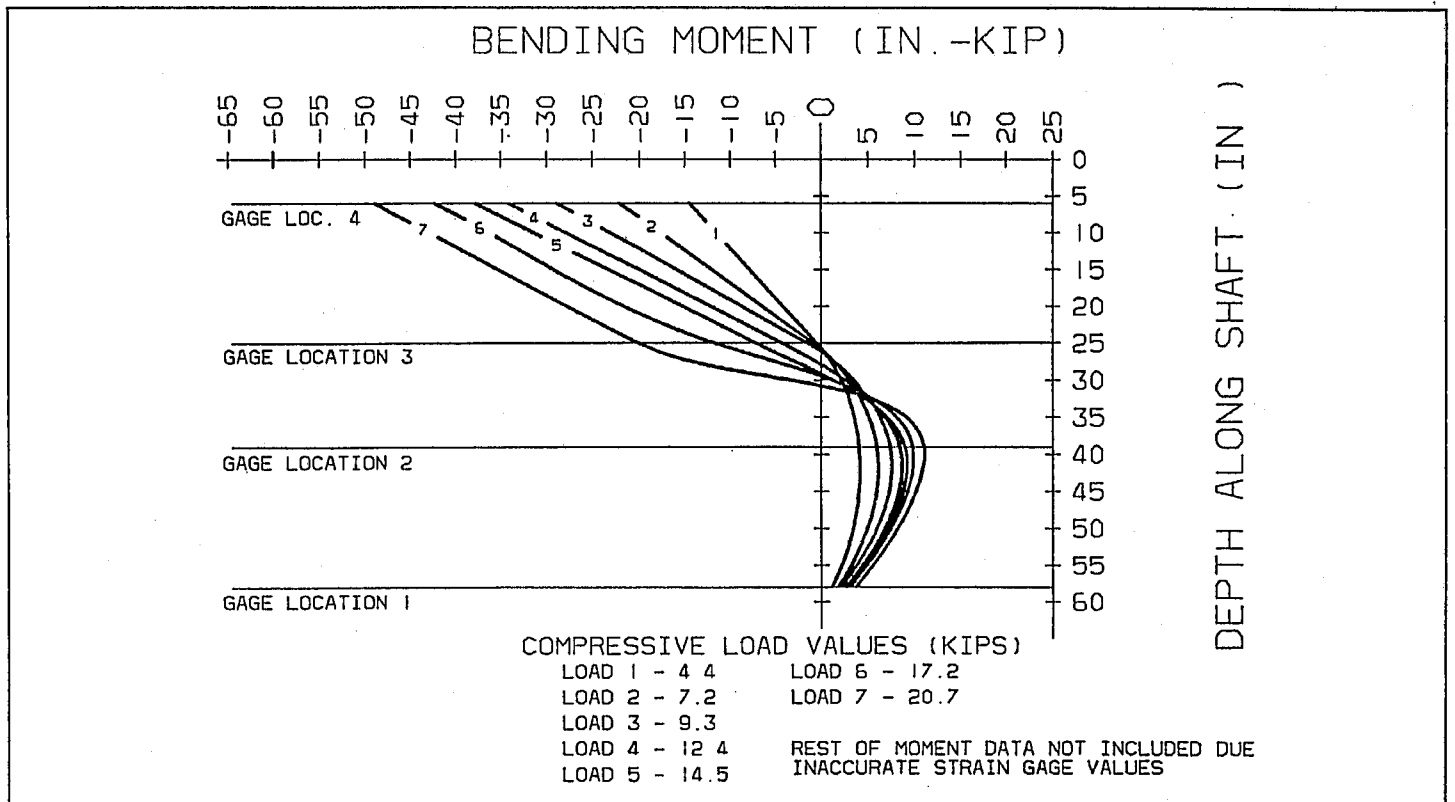
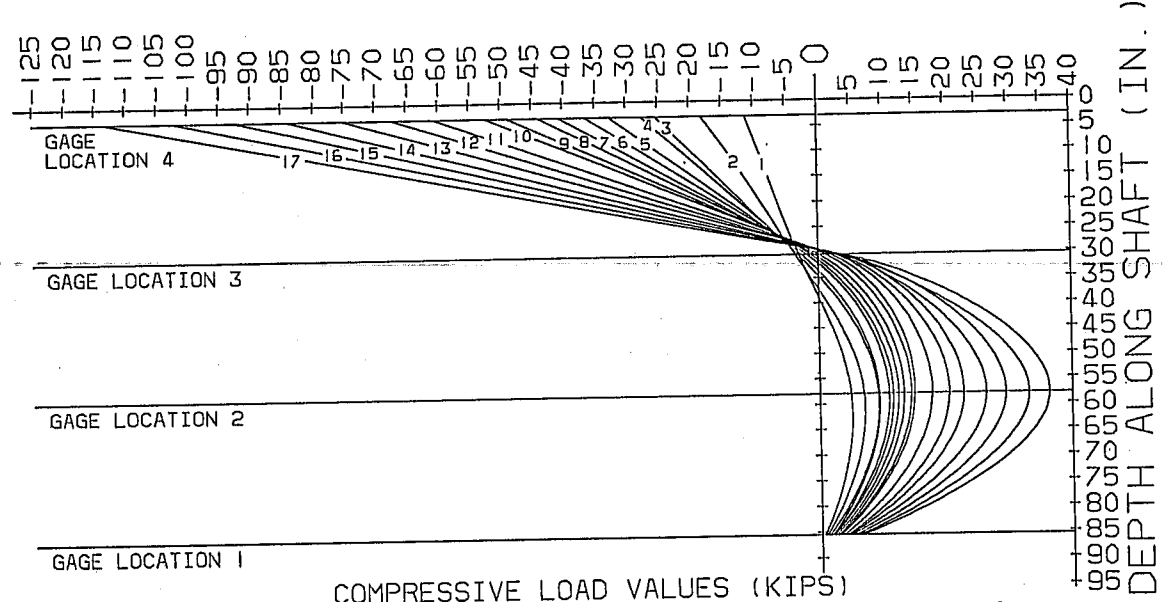


Fig. 5. SS150 Helical Pier

## BENDING MOMENT (IN.-KIP)



COMPRESSIVE LOAD VALUES (KIPS)

LOAD 1 - 4.6	LOAD 6 - 21.5	LOAD 11 - 34	LOAD 16 - 46.9
LOAD 2 - 10	LOAD 7 - 23.8	LOAD 12 - 36.6	LOAD 17 - 49.3
LOAD 3 - 14.5	LOAD 8 - 24.6	LOAD 13 - 38.1	
LOAD 4 - 15.8	LOAD 9 - 28.5	LOAD 14 - 40.5	
LOAD 5 - 19.4	LOAD 10 - 30.5	LOAD 15 - 43.8	

Fig. 6. SS175 Helical Pier

Figure 5, which shows the results of the SS150 pier, does not include several additional load cases. The reason for this is that problems with the strain gages during field tests created inaccurate results.

Stress analysis can be conducted directly from the moment-depth curves. By calculating total stress at any given point and comparing it with the strength of the shaft material, initial yield conditions can be determined. The curves show that the largest factor contributing to total stress is the bending moment, at least within the length of the top pier extension. However, the moment-depth curves indicate that applied moments at the top of the pier are dissipated by passive soil pressure along the shaft, and that the dissipation occurs along a relatively short distance of the pier. At any point below this dissipation zone, the major factor contributing to total stress is the axial load. As previously stated, axial loads for underpinning will typically be between 6 and 15 kips. These loads by themselves will not produce an axial stress in the pier shaft that is large enough in magnitude to cause a yield condition. Thus, the region of critical stress along the pier shaft appears to be the top 6' to 10', depending on the pier type.

Table 3 lists the actual mechanical properties of the steel used in the pier shafts. This data is given for comparison between total stress during tests and strength of material used. The values listed in Table 3 are not necessarily typical values. They are shown for direct comparison of actual test data.

Table 3. Mechanical Properties of Shaft Material

Pier Type	Yield Strength (KSI)	Ultimate Strength (KSI)
SS5	69	110
SS150	107	141
SS175	96	136

Table 4 lists the compressive loads required to approximate a yield condition on the outer fibers of the shaft. The first column lists loads where the total extreme fiber stress  $\sigma$  is a compressive stress. In other words, it is the stress on the face of the pier shaft oriented toward the footing of the building. The second column lists loads where the total extreme fiber stress is a tensile stress. This occurs on the face of the pier shaft opposite the face with compressive stress. The two values are different for a given pier type because the axial load produces a compressive stress only.

Table 4. Compressive Loads at Yield

Pier Type	Load at $\sigma_c = S_y$ (Kips)	Load at $\sigma_t = S_y$ (Kips)
SS5	16	18
SS150	21	25
SS175	38	44

The bending moments used in Table 4 come from gage location 4, which was the nearest to the surface. This was where the recorded bending moment was highest. As mentioned before, strain gages will work up to the elastic limit. Therefore, loads and moments recorded that were higher than the values used in Table 4 cannot be considered accurate and should not be used. This is true only at gage location 4.

Angular deflection data obtained during load tests show that the steel bracket does rotate due to the eccentric load. The stiffness of the steel bracket and concrete footing help to keep the rotation reasonably low. The direction of rotation always tends to move the top of the bracket toward the building. Table 5 lists the rotation angles of the steel brackets with respect to the footing.

Table 5: Angular Rotation of Steel Bracket

Pier Type	Max. Load (Kips)	Max. Rotation (Degrees)
SS5	24.2	5.85
SS150	36	5.54
SS175	50	3.65

The only pier shaft that suffered any permanent damage was the SS5 shaft. Eighteen inches below the top, the shaft was bent about 3° in a direction toward the building. The 18" is the exact amount of shaft length that the steel bracket covers on the 1½" piers. Thus, the shaft bent in the area just below the bracket. This corresponds to the area of highest bending moment.

## DISCUSSION OF TEST RESULTS

Test results show that bending moments along the pier shaft dissipate over a relatively short distance. For example, on the SS5 pier, the bending moment corresponding to the maximum load applied (24.2 kips) was only about 6 in-kip at a depth of 62". Recall that the entire pier length was about 17'.

The same can be said for the SS150 and SS175 piers. SS150 data shows that at a load of 21 kips, the bending moment was about 4 in-kip at 62" depth. Overall pier length was about 22'. As for the SS175, a bending moment of about 7 in-kips was measured at 85" depth at a maximum load of 50 kips. Overall pier length was about 21'.

The moment-depth curves shown in Figures 4, 5, and 6 suggest that the bending moment would dissipate completely. However, there is no way of knowing with just the strain gage data presented.

In order to verify the test results, a pile analysis program called LPILE was used. LPILE is a product of Ensoft, Inc. in Austin, Texas. LPILE is a finite difference program for pile analysis. With it, theoretical moment versus depth curves were made for comparison. Results show similar moment versus depth profiles, but the predicted moments are less than

the moments measured in the field. This is due probably in part to the fact that the soil strength parameters taken from Table 1 were used to model the soil. Table 1 data for cohesion and unit weight was obtained from soil at depths well below the bending moment dissipation zone. Another possible reason for the difference in actual versus predicted moments was the fact that the soil was slightly remolded around the shaft due to the passage of the helices during installation. LPILE does show that the bending moment dissipates to zero in a relatively short distance.

## CONCLUSIONS

This test series has shown that Helical Piers can be used successfully for underpinning residential and light commercial structures. Eccentric compression loading creates a bending moment in the pier shaft below the steel bracket at the top of the pier. This moment is highest directly below the bracket, but dissipates in a relatively short length. Passive soil pressures along the shaft dissipate the bending moment. From this observation, it is reasonable to expect a stiffer soil to be able to dissipate higher bending moments developed from higher compressive loads.

The slenderness of the pier shaft and its ability to withstand combined axial and bending stress is a primary concern when selecting a pier type. A pier should not be selected only on the basis of the required design load and expected torque requirement. The ability of the soil to passively dissipate bending moments must also be considered. Design loads, required torque, and bending moment capacity are the primary variables in pier selection. That is why three different types of Helical Piers were tested. A choice can be made as to which pier would best suit the needs of a specific underpinning project. Proper installation techniques are equally important to the behavior of Helical Piers. Placing the pier shaft as close to the grade beam or footing as possible will minimize the offset between the pier and the load center.

Proper shaft orientation, as shown in Figure 3a, will ensure that the pier shaft will have its maximum natural bending capacity. In addition, a steel bracket that has been properly seated and bolted to the footing or grade beam will ensure that the top of the pier is rigid and has greater resistance to deflection under load. A pile that has its top rigidly fixed is less likely to buckle than a pile that is pinned or free at the top.

All axial load and bending moment data presented in this paper was based on strain gage information. Due to the nature of the environment to which the gages were subjected, some degree of error should be expected. One way to check this error was to compare axial loads as determined by strain gages, and loads as shown by the calibrated hydraulic pumps. For example, the average % error between calibrated pump and gage for the SS150 pier was 18%. However, the average % error for the SS175 pier was only 5%. This indicates that the SS150 data is questionable.

Based on these conclusions, additional testing should be done to verify the results, preferably at different test sites with different soil profiles.

#### Symbols in order of Appearance

N	-	blow count
W	-	water
LL	-	liquid limit
PL	-	plastic limit
PI	-	plasticity index
C	-	cohesion of soil
$\epsilon$	-	axial strain at failure
$\gamma_d$	-	unit dry weight
$\sigma_c$	-	total compressive stress
$\sigma_t$	-	total tensile stress
Sy	-	yield strength

#### References

Chance Company, 1992. Basic Guidelines for Designing Helical Piers for Underpinning, Bulletin 01-9202, Centralia, Missouri.

Clemence, S.P. and Hoyt, R.M., 1989. Uplift Capacity of Helical Anchors in Soil, International Conference on Soil Mechanics and Foundation Engineering, Rio de Janeiro, Brazil, pp 1019-1022.

Edwards, W.G. and Rupiper, S., 1989. Helical Bearing Plate Foundations for Underpinning, ASCE Foundation Engineering, Proceeding of the Congress, Evanston, Illinois, pp 221-230.

Hargrave, R.L. and Thorsten, R.E. Helical Piers in Expansive Soils of Dallas, Texas, 7th International Conference on Expansive Soils, Dallas, Texas, pp 125-130.